

Live axonal transport disruption by mutant huntingtin fragments in *Drosophila* motor neuron axons

C. Sinadinos^a, T. Burbidge-King^a, D. Soh^a, L.M. Thompson^{d,e,f}, J.L. Marsh^{b,c},
A. Wyttenbach^{a,*}, A.K. Mudher^{a,*}

^a School of Biological Sciences, University of Southampton, Bassett Crescent East, Southampton SO14 7PX, UK

^b Department of Developmental and Cell Biology, University of California, Irvine, CA 92697, USA

^c Department of Pathology, University of California, Irvine, California 92697, USA

^d Department of Psychiatry and Human Behavior, University of California, Irvine, CA 92697, USA

^e Department of Neurobiology and Behavior, University of California, Irvine, CA 92697, USA

^f Department of Biological Chemistry, University of California, Irvine, CA 92697, USA

ARTICLE INFO

Article history:

Received 14 November 2008

Revised 16 February 2009

Accepted 21 February 2009

Available online 4 March 2009

Keywords:

Huntington's Disease
N-terminal huntingtin
Drosophila
Motor neurons
Axonal transport
neuropeptide-Y
Locomotion behaviour
Environmental stress

ABSTRACT

Huntington's Disease is a neurodegenerative condition caused by a polyglutamine expansion in the huntingtin (Htt) protein, which aggregates and also causes neuronal dysfunction. Pathogenic N-terminal htt fragments perturb axonal transport *in vitro*. To determine whether this occurs *in vivo* and to elucidate how transport is affected, we expressed htt exon 1 with either pathogenic (HttEx1Q93) or non-pathogenic (HttEx1Q20) polyglutamine tracts in *Drosophila*. We found that HttEx1Q93 expression causes axonal accumulation of GFP-tagged fast axonal transport vesicles *in vivo* and leads to aggregates within larval motor neuron axons. Time-lapse video microscopy, shows that vesicle velocity is unchanged in HttEx1Q93-axons compared to HttEx1Q20-axons, but vesicle stalling occurs to a greater extent. Whilst HttEx1Q93 expression did not affect locomotor behaviour, external heat stress unveiled a locomotion deficit in HttEx1Q93 larvae. Therefore vesicle transport abnormalities amidst axonal htt aggregation places a cumulative burden upon normal neuronal function under stressful conditions.

© 2009 Elsevier Inc. All rights reserved.

Introduction

Neurodegeneration in Huntington's Disease (HD), caused by an N-terminal polyglutamine (polyQ) expansion within the huntingtin (Htt) protein (The Huntington's Disease Collaborative Research Group, 1993), involves progressive death of neurons in the striatum and cortex (Reiner et al., 1988). As clinical progression can precede extensive neuronal death (Vonsattel et al., 1985), focus has centred on early pathological events that disrupt neuronal function prior to neuronal demise. Axonal dysfunction may represent one such event, as post mortem brain tissue from pre-symptomatic HD sufferers exhibits axonal degeneration of striatal projection neurons (Albin et al., 1992) and cortico-striatal afferents (Sapp et al., 1999). Dystrophic neurites, and swellings of accumulated cargoes indicative of axonal transport disruption, have been localised to aggregated htt inclusion bodies

(IBs), a common biomarker for HD neuropathology (DiFiglia et al., 1997). Axonal abnormalities have also been described in pre-symptomatic HD mice expressing the first exon of htt (HttEx1) with a polyQ expansion (Wade et al., 2008). Analysis of pathogenic human htt effects on axonal transport in transgenic animal models (Li et al., 2001; Gunawardena et al., 2003; Lee et al., 2004; Trushina et al., 2004) demonstrates that a functional htt deficit and its aggregation into axonal IBs, which impede transport and sequester motor components, may be key pathogenic events. Whilst end-point indications of axonal transport disruption are intriguing, dynamic events underlying perturbation have, to date, only been assessed *in vitro* (Szebenyi et al., 2003; Trushina et al., 2004; Orr et al., 2008), prompting the development of animal models to analyse such phenomena in a less biologically artificial environment *in vivo*.

Transgenic expression of pathogenic HttEx1 induces HD-like pathology in mice (Mangiarini et al., 1996) and neurotoxicity in *Drosophila* (Steffan et al., 2001). Furthermore pan-neuronal expression of polyQ-expanded HttEx1 in *Drosophila* induces the accumulation of axonal transport cargoes within motor and sensory axons of the major larval peripheral nerves *ex vivo* (Gunawardena et al., 2003). Whilst previous work has utilised the pliable genetics of *Drosophila* to further understand

* Corresponding authors. Fax: +44 2380594459.

E-mail addresses: aw3@soton.ac.uk (A. Wyttenbach), a.mudher@soton.ac.uk (A.K. Mudher).

Available online on ScienceDirect (www.sciencedirect.com).

transport disruption, demonstrating a reduced pool of functional transport motors (Gunawardena et al., 2003), mutant htt transport perturbation remains unconfirmed in live animals and dynamic events occurring prior to cargo accumulation have yet to be probed directly.

Here, we describe a new model of mutant HttEx1 axonal pathology in which both expanded HttEx1 and a fluorescent axonal transport reporter protein are expressed specifically in *Drosophila* motor neurons, and result in somal and axonal HttEx1 aggregation. Real-time axonal vesicle stalling and cargo accumulation is observed in live, intact larvae for the first time in an HD animal model. By assaying the consequences of mutant htt expression for larval behaviour we show that transgenic larvae move normally but exhibit a marked locomotor deficit following additional external heat stress. This model will contribute towards an understanding of pathological axonal transport events arising due to an interplay between N-terminal htt toxicity and environmental stressors in HD.

Results

Mutant HttExon1 aggregates within *Drosophila* motor neuron axons

To understand the effects of pathogenic htt on axonal transport, a human HttEx1 fragment comprising of 63 N-terminal amino acids, flanking a non-pathogenic (HttEx1Q20) or pathogenic length (HttEx1Q93) polyQ tract (Steffan et al., 2001), was expressed in *Drosophila* motor neurons with the *D42-GAL4* driver. N-terminal htt, consistent with the size of HttEx1, is cleaved during HD pathology and found in HD inclusion bodies (IBs) in human brain (Zhou et al., 2003). As axonal mutant HttEx1 aggregates may contribute to transport disruption (Gunawardena et al., 2003), we studied the axonal distribution of HttEx1 in fixed motor neuron axons within the peripheral nerves of dissected larvae. Immunohistochemistry with the S830 antibody, directed at the N-terminus of human htt (Sathasivam et al., 2001), reveals characteristic HttEx1 accumulation in the nerves of HttEx1Q20 and HttEx1Q93 larvae raised at 23 °C that is absent in Oregon R (OreR) wild-type controls (Figs. 1A, B). Staining is not observed upon omission of primary antibodies (Fig. S1). Annular (Fig. 1Ai) or spherical (Fig. 1Aii) aggregates of HttEx1 that exceed 1.3 µm in diameter, classed as large aggregates (LAg), are present in larval nerve in this model (Figs. 1A–E; Fig. S2) (refer to materials and methods for further details on classification of aggregates). LAg are significantly elevated in HttEx1Q93 larvae raised at 23 °C relative to OreR (Fig. 1B, C, $p < 0.05$, $n = 5$) and there is a trend towards increased LAg in HttEx1Q93 versus HttEx1Q20 (Fig. 1C, $p = 0.13$). Small aggregates (SAg) with a diameter below 1.3 µm (Fig. 1Aiii), or tracks (TRs) that appear to run along a single axon (Fig. 1Aiv), are unchanged in HttEx1Q93 larvae relative to HttEx1Q20 (Fig. 1C). EM48 antibody, which reacts with HttEx1 and is relatively selective towards aggregated htt species (Zhou et al., 2003), reveals a significantly greater number of SAg structures in HttEx1Q93 nerves (Figs. 1D, E, $p < 0.001$, $n = 4$), although LAg are rare (Fig. 1E). HttEx1 aggregate-like structures thus form within the nerves of HttEx1Q20/Q93 larvae detected with two different antibodies, with an increase of SAg in mutant larvae detected by the EM48 antibody.

As UAS-GAL4 transgene expression can be temperature-sensitive (Phelps and Brand, 1998), HttEx1Q93 larvae raised at 23 °C may display moderate levels of htt aggregation due to low mutant transgene expression levels. We thus investigated the effect of raising larvae at 29 °C on the axonal distribution and expression levels of HttEx1Q93. HttEx1Q93 larvae raised at 29 °C show a striking increase in LAg, SAg and TR numbers, as detected with S830 antibody in peripheral nerves, with all accumulate types significantly more prevalent compared to HttEx1Q20 controls (Figs. 1F, G, LAg $p < 0.001$, SAg $p < 0.01$, TR $p < 0.01$, $n = 5$). When HttEx1Q93 larvae raised at 29 °C are analysed with EM48 antibody (Fig. 1H), LAg are 8 times more prevalent than in HttEx1Q20 (Fig. 1I, $p < 0.05$, $n = 3$). To further define

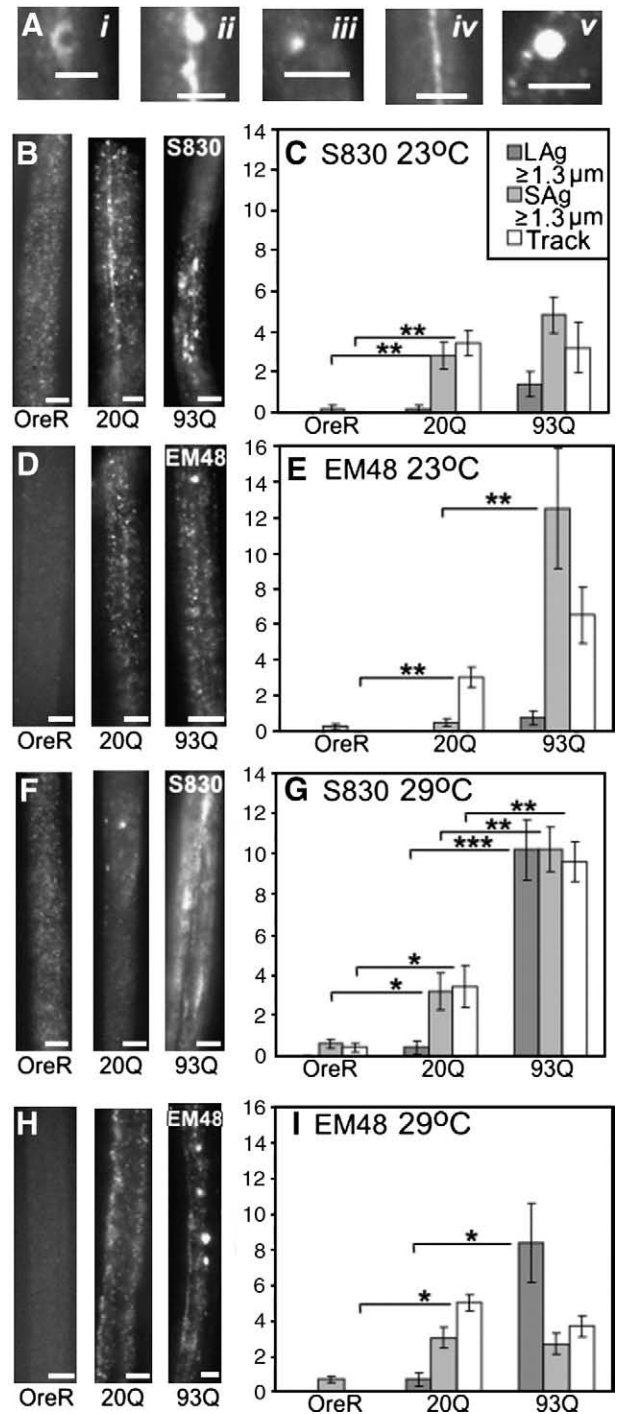


Fig. 1. Axonal Htt distribution and aggregation in *Drosophila* motor neuron axons. (A) Representative structures detected with anti-HttEx1 (S830) and anti-Htt aggregate (EM48) antibodies in larvae expressing HttEx1-polyQ in motor neurons. S830 (i) annular or (ii) dense large aggregate (LAg); (iii) small aggregate (SAg); (iv) track (TR); (v) EM48 large aggregate (LAg). The typical distribution of HttEx1, detected with S830, in wild-type OreR, HttEx1Q20 and pathological HttEx1Q93 axons is shown for animals raised at 23 °C (B) and 29 °C (F). 5 larvae were analysed for each genotype. Typical Htt EM48 aggregate immunoreactivity for animals raised at 23 °C (D) and 29 °C (H) is also shown. Q93 animals raised at 23 °C possess more LAg than controls (E). This trait is exacerbated in Q93 animals raised at 29 °C (I), in which SAg and TRs are also elevated. Q93 larvae raised at 23 °C display more EM48 SAg than controls (E), whereas animals raised at 29 °C display fewer SAg but more LAg (I). For each genotype, 4 larvae raised at 23 °C and 3 raised at 29 °C were analysed. Statistically significant differences for relevant comparisons are indicated by stars * $p < 0.05$; ** $p < 0.01$; *** $p < 0.001$. Non-significance is not indicated. Scale bars are 3 µm (A) and 5 µm (B, D, F and H).

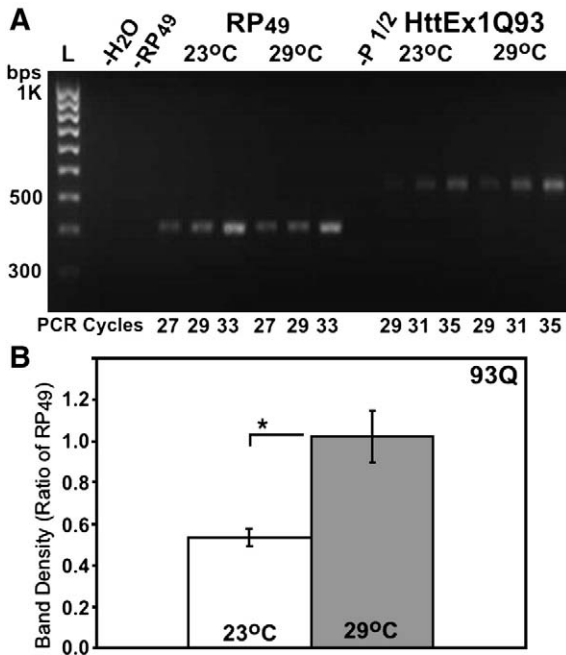


Fig. 2. Semi-quantitative RT-PCR of HttEx1 from HttEx1Q93 total RNA. (A) HttEx1Q93 product bands are detectable for larvae raised at both 23 °C and 29 °C. RNA for ribosomal protein RP49 was used as an RNA baseline control. –H₂O – water negative control, –RP49 – RP49 negative PCR control, –P1/2 – HttEx1Q93 negative PCR control. (B) Band density analysis indicates that animals raised at 29 °C show a significantly greater level of transgene expression than those raised at 23 °C ($p < 0.05$, $n = 3$ crosses).

axonal aggregate dimensions, we collected Z-stack confocal images of EM48 immunoreactivity in HttEx1Q93 and HttEx1Q20 peripheral nerves (Fig. S2), confirming that Lag can span the 1–2 μm width of a normal peripheral larval axon (Hurd and Saxton, 1996; Gunawardena et al., 2003). We also analysed motor neuron cell bodies within the ventral nerve cord by this method. Mainly nuclear EM48 immunoreactive aggregates are present in HttEx1Q93 larvae, but were not found in control animals (Fig. S2). Analysis of nuclei by Hoechst staining (Figs. S2J–L), no difference in the number of detectable neuromuscular junctions (Fig. S3), and no significant change in the overall diameter of peripheral nerves (data not shown) across the three genotypes, argues against cell loss in HttEx193Q versus HttEx1Q20 ventral cord.

To compare HttEx1Q93 transgene mRNA levels at both raising temperatures, we performed semi-quantitative rtPCR on larval total RNA (Fig. 2A). Analysis of the resultant HttEx1Q93 band, absent in controls, indicates a significant elevation in expression at 29 °C versus 23 °C (Fig. 2B, $p < 0.05$, $n = 3$). HttEx1Q93 accumulation and aggregation may thus be concentration dependent in *Drosophila* larval motor neuron

Table 1
In vivo vesicle dynamics in larval peripheral nerve.

	Average velocity ($\mu\text{m s}^{-1}$)	Average velocity (VS) ($\mu\text{m s}^{-1}$)	Maximum velocity (VM) ($\mu\text{m s}^{-1}$)	Stalls (/region)	Circulatory motion (/region)
OreR	0.93 ± 0.02	0.87 ± 0.03	1.11 ± 0.04	1.08 ± 0.39	0.25 ± 0.12
20Q	0.89 ± 0.04	0.82 ± 0.04	1.06 ± 0.07	1.33 ± 0.28	$0.75 \pm 0.22^*$
93Q	0.93 ± 0.04	$0.79 \pm 0.03^\dagger$	1.13 ± 0.06	$2.75 \pm 0.54^*$	$0.83 \pm 0.27^*$

4 separate nerve regions were analysed from each of 3 larvae, and 5 vesicles analysed within each region. Average velocity includes travel in anterograde and retrograde directions and excludes stalls. VS is the average velocity for all vesicles and includes stalling events. VM is the maximum velocity for any vesicle in each region. Stalls were defined as pauses in vesicle locomotion during which less than 0.2 μm was attained within 1 s, and “circulatory motion” as local successive oscillatory changes in vesicle direction. Errors indicate SEMs.

Significance within a column (*) or row (†) is indicated ($p < 0.05$, $n = 12$ regions).

axons, although other chronic effects of a higher raising temperature on htt axonal localisation and/or aggregation state cannot be ruled out.

Expanded HttEx1 perturbs axonal transport in vivo

To assess whether axonal HttEx1Q93 accumulation and aggregation perturbs axonal transport within intact live *Drosophila*, we utilised double transgenic HttEx1Q93 larvae that co-express a human neuropeptide-Y-GFP fusion protein (vGFP) in motor neurons. Neuropeptide-Y is a fast axonal transport cargo (D’Hooge et al., 1990), and vGFP is diffusely distributed in wild-type nerve but accumulates into large deposits within the axon when transport is compromised in a *Drosophila* model of tauopathies (Mudher et al., 2004). Whilst vGFP accumulates are not visible in mutant htt larvae raised at 23 °C (Fig. 3C and data not shown), the peripheral nerves in mutant htt larvae raised at 29 °C show a 2-fold increase in total vGFP accumulate area relative to HttEx1Q20 larvae (Figs. 3A, B, $p < 0.05$, $n = 6$).

To investigate the mechanism by which vGFP accumulates in axons of HttEx1Q93 larvae, we analysed dynamic vesicle movement along the peripheral nerves of intact anaesthetised larvae raised at 29 °C. We observed both continuously moving and stalling vesicles, which pause for significant time periods, in larval nerves (see Movies M1, M2, and M3, Supplementary material). When stalling vesicles are excluded from analysis, the average and maximum velocity of uninterrupted vesicle transport along several separate regions of nerve is not reduced upon HttEx1Q93 expression (Table 1). However, stalling of vGFP vesicles is significantly increased in HttEx1Q93 nerves (Table 1, $p < 0.05$, $n = 12$ regions), and average velocity of all vesicles, including stalling vesicles, is reduced in HttEx1Q93 nerves (Table 1, $p < 0.05$). A peculiar “circulatory” motion of vesicles, involving repeated switches between anterograde and retrograde movement, occurred more frequently in both mutant and wild-type htt larvae relative to OreR controls (Table 1, $p = 0.08$, $n = 12$ regions).

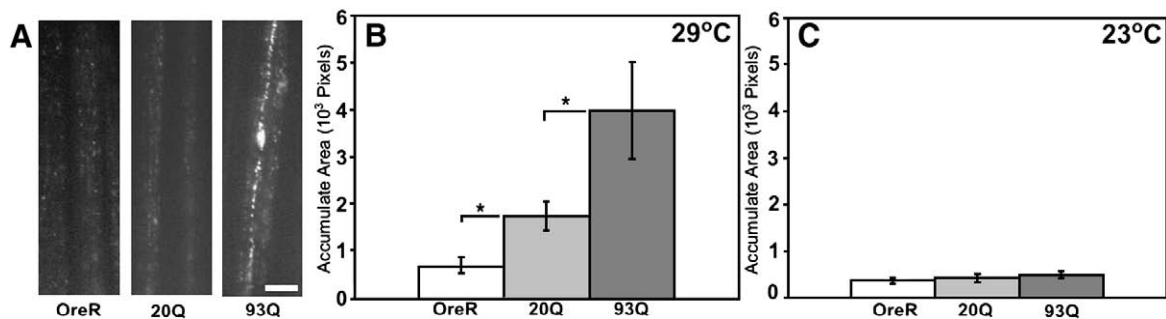


Fig. 3. In vivo axonal cargo accumulation in HttEx1Q93 expressing *Drosophila*. (A) Representative vesicular neuro-peptide-Y-GFP (vGFP) distribution in larval peripheral nerves. Live, immobilised HttEx1Q93 specimens show extensive axonal accumulation of vGFP fluorescence, whereas vGFP in control nerve is distributed diffusely. Scale bar – 5 μm . (B) Relative total vGFP accumulate area, quantified over a restricted region of peripheral nerve, reveals a progressive increase in vGFP accumulation with increasing polyQ length for larvae raised at 29 °C. (C) Constant low level fluorescence in HttEx1Q93 and controls raised at 23 °C. 6 larvae raised from a single cross were analysed for each genotype ($p < 0.05$).

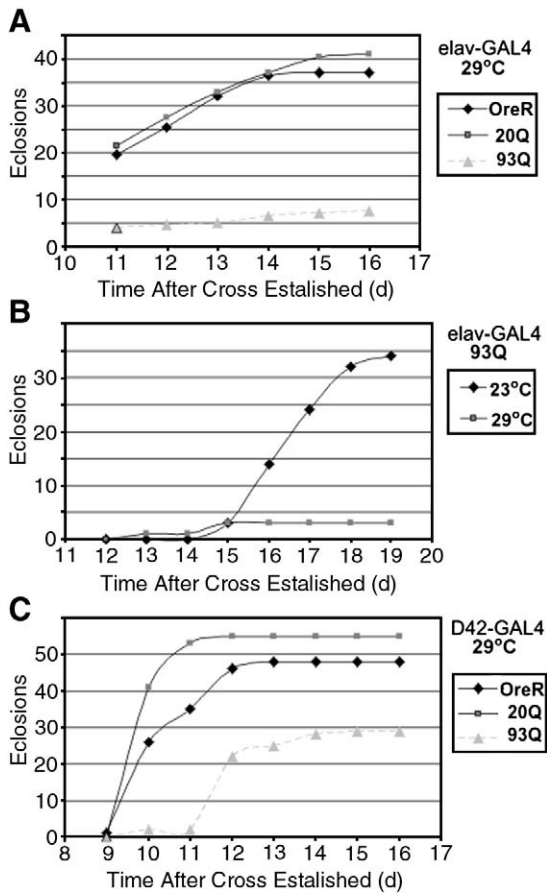


Fig. 4. Developmental effects of HttEx1Q93 expression in *Drosophila*. (A) Number of adult eclosures after pan-neuronal transgene expression at 29 °C. HttEx1Q93 expression is severely toxic, preventing development to adult of all but a few specimens, whereas OreR and HttEx1Q20Q controls develop normally. (B) HttEx1Q93 animals raised at 23 °C develop normally into adults. (C) HttEx1Q93 expression in motor neurons allows some larvae to reach adulthood but causes a developmental delay. 6 pUAS transgenic males were crossed to 10 driver females in a single test cross for each genotype.

Data in Table 1 are derived from analysis of movies as illustrated and described in detail in Supplementary material. These results demonstrate that HttEx1Q93 expression disrupts axonal transport in different ways: it increases retention of transport vesicles (accumulates) in the axon, and promotes stalling of motile vesicles.

Neuronal function is impaired by pathogenic HttEx1

To assess whether HttEx1Q93 expression detrimentally affects neuron function, mutant HttEx1 was expressed pan-neuronally using the *elav-GAL4* driver. *Drosophila* pupation and metamorphosis, prior to emergence (eclosion) as a pharate adult, is a period of intense physiological change and sensitivity to toxic insult. Previous work indicates that pan-neuronal HttEx1Q93 toxicity in *Drosophila* allows only 20–30% of embryos to eclose (Steffan et al., 2001; Wolfgang et al., 2005). Similarly, in our hands, 20.9% of HttEx1Q93 larvae raised at 29 °C eclose as adults relative to HttEx1Q20 (Fig. 4A). However, such a defect is not observed for HttEx1Q93 animals raised at 23 °C (Fig. 4B). When expression is directed to motor neurons at 29 °C, 52.7% of HttEx1Q93 larvae eclose as adults relative to HttEx1Q20, and development is delayed (Fig. 4C). Motor neuron-specific HttEx1Q93 expression thus subtly impedes development to adult eclosion, whereas HttEx1Q93 pan-neuronal expression more severely perturbs this stage in a temperature-dependent manner.

Heat shock unveils a behavioural phenotype in HttEx1Q93 larvae

In late L3-stage *Drosophila* larvae, body wall contraction capability and locomotion provides a direct, quantifiable readout of motor neuron function and behaviour. To quantify larval locomotion, we used contraction and line-crossing assays as previously described (Mudher et al., 2004). Surprisingly, HttEx1Q93 animals do not exhibit a significant reduction in contraction rate over 30 s when raised at either 23 °C or 29 °C (Figs. 5A, B). We also quantified the total number of lines crossed by each larva over a grid for 30 s, in a line-crossing assay that gauges free crawling ability. As with the contractions assay, HttEx1Q93 larvae raised at either temperature are not deficient in this line-crossing assay (Figs. 5C, D).

Although HD is a fully penetrant condition, environmental factors are likely to contribute to variations in clinical disease presentation (van Dellen et al., 2000; Wexler et al., 2004). Given that polyQ expression and external heat stress synergise to promote neuronal toxicity in *C. elegans* (Gidalevitz et al., 2006), we tested the effect of an acute heat shock prior to locomotion tests. When raised at 23 °C or 29 °C, all genotypes display a significant deficit in contraction rate and line-crossing ability following heat shock (Figs. 5A–D, $p < 0.01$, $n = 15$). However, the performance of the mutant htt larvae after heat shock in both assays is significantly reduced compared to HttEx1Q20 and OreR larvae when raised at 23 °C (Figs. 5A, B $p < 0.05$, $n = 15$) or 29 °C (Figs. 5C, D $p < 0.05$, $n = 5$). Interestingly, the

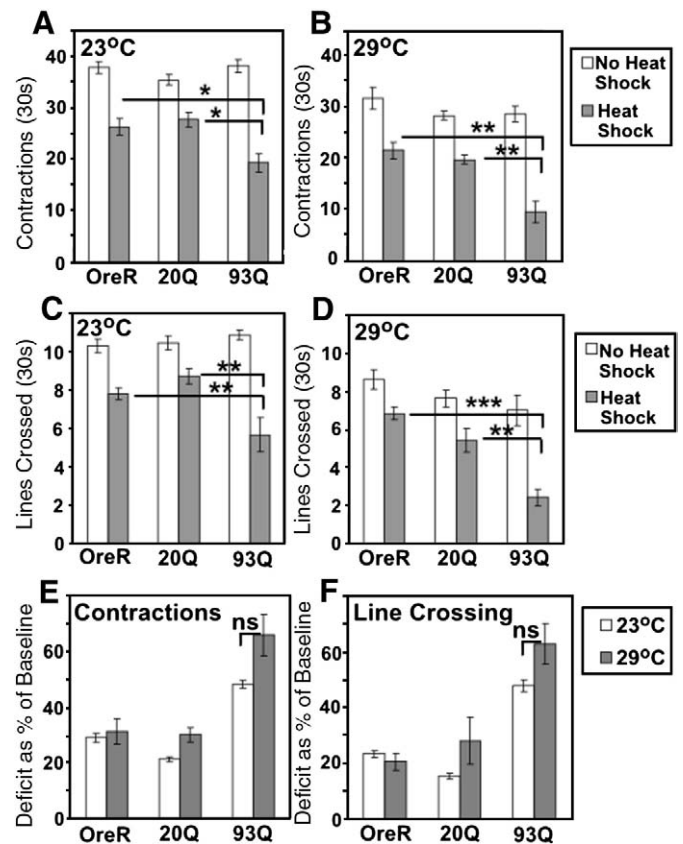


Fig. 5. Locomotion deficit in HttEx1Q93 expressing *Drosophila* larvae. (A) The number of body wall contractions over 30 s before (unstressed baseline) and after acute heat shock (HS) when raised at 23 °C. HttEx1Q93 animals complete fewer contractions than controls after HS only. This was also observed for larvae raised at 29 °C (B). (C,D) The number of lines crossed over a square grid for 30 s before and after acute HS. As for contractions, HttEx1Q93 animals raised at 23 °C (C) and 29 °C (D) cross fewer lines than controls after HS only. (E,F) Comparison of the relative post-HS locomotion deficit in HttEx1Q93 animals raised at 29 °C and 23 °C. 15 animals raised at 23 °C and 5 animals raised at 29 °C were tested for each genotype. Statistically significant differences for relevant comparisons are indicated by stars * $p < 0.05$; ** $p < 0.01$; *** $p < 0.001$. Non-significant, ns.

performance of HttEx1Q93 larvae reared at 29 °C showed a trend towards worse performance than HttEx1Q93 larvae reared at 23 °C (Fig. 5E, $p = 0.08$, 5F, $p = 0.13$, $n = 5$). Development to adult is normal for mutant HttEx1 animals and control animals exposed to acute heat shock (Fig. S4), arguing against a general fitness effect of heat shock on vulnerable HttEx1Q93 maturation and behaviour. Heat shock therefore reveals a specific behavioural phenotype in HttEx1Q93 larvae compared to HttEx1Q20 controls.

Discussion

We have shown that HttEx1Q93 expression perturbs axonal transport and neuronal function in larval *Drosophila* motor neurons *in vivo*. Axonal accumulation and aggregation of HttEx1Q93 correlates with transport disruption, which involves increased stalling and accumulation of GFP-labelled neuropeptide-Y transport vesicles. Our study is the first to perform such measurements in living animals using real-time analysis in an *in vivo* model of HD. Despite the transport impediment, we show that motor neuron-dependent larval locomotion appears normal unless animals are heat stressed prior to testing, which unveils a specific locomotor defect in mutant larvae. *In vivo* transport perturbation by pathogenic HttEx1 is thus one process by which pathogenic HttEx1 may weaken neuronal defences to external stress during HD pathology.

Although expressed and aggregated in the cell body, N-terminal htt-polyQ fragments (Li et al., 1999; Lee et al., 2004) or full length htt (Li et al., 2001) accumulate within axons in HD and in animal models. We show that axonal HttEx1Q93 EM48-immunoreactive aggregates (Figs. 1A–E; S2) can exceed the previously observed normal diameter of peripheral nerve axons (Hurd and Saxton, 1996). Observations of swollen peripheral nerves and retention of axonal transport cargoes has been reported in other polyQ *Drosophila* models (Gunawardena et al., 2003). As suggested previously, pathogenic polyQ containing proteins could disrupt axonal transport either by producing space-occupying aggregates within axons that physically impair transport, or by sequestering and/or interacting abnormally with various proteins involved in axonal transport (Gunawardena and Goldstein, 2005). Insoluble IBs isolated from human HD brain tissue are enriched for such proteins (Trushina et al., 2004), and transport cargo accumulation in expanded HttEx1Q93 *Drosophila* larval nerve is worsened by genetic reduction of motor proteins such as kinesin and dynein (Gunawardena et al., 2003). Transport disruption by N-terminal htt fragments could thus perturb axonal transport without microscopically visible aggregation. This has recently been shown in cell culture studies where expression of mutant HttEx1 results in mitochondrial transport defects in the absence of obvious aggregate formation (Orr et al., 2008). Interestingly, pan-neuronal Htt-full-length-Q128 expression in *Drosophila* did not result in detectable aggregation or transport cargo accumulation within the larval peripheral nerves (Romero et al., 2008).

Our novel approach to visualize real-time axonal transport in living intact larvae shows that continuously moving GFP-tagged vesicles travel along HttEx1Q93 nerve at a velocity of $0.93 \pm 0.04 \mu\text{m/s}$ (Table 1), consistent with the lower limit of fast axonal transport (Brown, 2003). This value contrasts with an acute 25–30% reduction in transport vesicle velocities following perfusion of pathogenic N-terminal htt fragments over isolated squid axoplasm (Szebenyi et al., 2003). This discrepancy with our findings could be due to our exclusion of stalling vesicles in our calculations of average velocity. When such vesicles were included in our velocity calculation in addition to the continuously moving GFP-tagged vesicles, the average velocity was significantly reduced in HttEx1Q93 nerve to $0.79 \mu\text{m/s}$, which was not the case for OreR or HttEx1Q20 control nerve (Table 1). These results highlight the importance of stalling events: more stalling events were observed in HttEx1Q93 nerve (Table 1), and this is in agreement with an increase in ‘stop-go’ vesicular motion

detected in axons of cultured primary striatal neurons derived from Htt-FLQ72 knock-in mice (Trushina et al., 2004). It is possible that GFP-tagged vesicles detach from fully active motor proteins during stalling, particularly if there is a total motor protein deficit due to local sequestration to htt aggregates, and thus excessive competition with other fast axonal transport cargoes in HttEx1Q93 axon. Consistent with this notion, GFP-tagged vesicles accumulate in the motor axon upon HttEx1Q93 expression (Figs. 3A, B).

Accumulation of GFP-tagged vesicles has been reported in a *Drosophila* model of Tauopathies, following the expression of human tau (Mudher et al., 2004). Despite axonal transport alterations in this tau model, the larval neuromuscular junctions (NMJs) were present and no cell loss in the ventral cord was detected, suggesting that these transport defects are not a consequence of neuronal loss (Mudher et al., 2004). Analysis of NMJs in mutant HttEx1 versus HttEx1Q20 larvae revealed no difference (Fig. S3), suggesting that the axonal transport disruption in mutant htt larvae is not a consequence of neuronal cell death (with associated NMJ loss), but rather a consequence of neuronal dysfunction. It is possible that the axonal transport defects that we observe could be due to nuclear events (such as abnormal transcription), as HttEx1Q93 aggregates were also found in the motor neuron nuclei (Fig. S2). Interestingly, a reversible defect in retrograde axonal transport was found to correlate with androgen receptor-polyQ (AR-97Q) nuclear aggregate formation and reduced expression of dynactin-1 in a mouse model of spinal and bulbar muscular atrophy (Katsuno et al., 2006). This is consistent with transport being affected by pathological changes in the nucleus. When perfused over isolated squid axoplasm *in vitro*, however, pathogenic AR-57Q also reduced axonal transport vesicle velocity in a similar manner to N-terminal htt (Szebenyi et al., 2003), suggesting a direct interference of transport in the axon. This was more recently attributed to an alteration in regulatory signalling pathways on axonal transport by soluble AR-57Q (Morfini et al., 2006). Perturbation of axonal transport may be a common pathogenic mechanism amongst polyQ disorders, as axonal aggregation of spinocerebellar ataxia 3 protein with a pathogenic polyQ tract (SCA3-78Q) in *Drosophila* larval motor neurons was associated with defective axonal transport of vesicular cargoes (Gunawardena et al., 2003), although this was concurrent with extensive motor neuron cell death and other work has shown that SCA3-78Q is prone to nuclear aggregation rather than accumulation in the axon to disrupt transport in this model (Lee et al., 2004).

Despite previous work showing that defective axonal transport in *Drosophila* motor neurons can perturb larval motor neuron function and locomotion (Hurd and Saxton, 1996; Mudher et al., 2004), HttEx1Q93 larvae do not show defective locomotion under normal environmental conditions, even if they are reared at high temperature (29 °C). This could be due to compensatory cellular mechanisms in the axonal compartment. Individuals with genetically equivalent htt-polyQ expansions show considerable variation in their neuropathological manifestation of HD and environmental factors are showing an emerging clinical significance in HD pathology (Wexler et al., 2004). Furthermore, environmental stress can influence pathology in HD rodent and *C. elegans* models (van Dellen et al., 2000). One environmental stress with relevance to protein conformational disorders is heat shock: work with temperature-sensitive mutants in *C. elegans* demonstrated that htt-polyQ misfolding synergises with heat shock to perturb the function of ‘metastable’ proteins in the neuron (Gidalevitz et al., 2006). Hence, we applied stress in the form of heat shock prior to locomotion assays and found that prior acute heat shock uncovers a defective locomotor phenotype in mutant larvae. These findings demonstrate that protein misfolding and aggregation, due to expression of mutant HttEx1Q93, sensitises neurons to external stressful stimuli *in vivo*, unveiling behavioural phenotypes that would not otherwise be apparent.

A molecular dissection of neuropathology in this *Drosophila* model could reveal how axonal transport fails in HD. Furthermore, this model

will allow exploration of how intrinsic htt-polyQ and extrinsic environmental pressures converge to override various cellular protection mechanisms and perturb essential aspects of neuronal function, giving rise to functional deficits observed in the human condition.

Materials and methods

Drosophila genetics

Transgenic expression of Htt-polyQ was directed to *Drosophila melanogaster* motor neurons via use of the pUAS-GAL4 system (Brand and Perrimon, 1993). Male flies homozygous for UAS-Htt-exon1-93Q, or UAS-Htt-exon1-20Q control, were crossed to neuropeptide-Y (vGFP) and D42 driver (vGFP-D42) homozygous female virgins, as described previously (Mudher et al., 2004). Oregon R homozygous males not carrying a pUAS insert were crossed to vGFP-D42 virgins as a driver control (OreR). UAS lines were also crossed to *elav* pan-neuronal driver female virgins. F1 L3-stage larvae were selected by size and wandering behaviour for analysis. Crosses were raised at 23 °C or 29 °C on a standard medium of corn meal, yeast and agar (Mudher et al., 2004).

Immunohistochemistry and Hoechst analysis

L3 larvae were dissected with a microdissection apparatus (Fine Science Tools, Interfocus, UK) under a WM light microscope (Heerberg, Switz.) in ice-cold *Drosophila* saline to reveal nervous tissue. Dissected preparations ('skins') were fixed in 4% paraformaldehyde for 90 min, before a 10 min wash in PBS containing 0.1% tween (0.1% tPBS). Skins were incubated for 30 min in 2 N HCl prior to 4 washes in tPBS. Skins were blocked for 30 min (30 µl/ml horse serum in 0.1% tPBS) before incubation in the primary antibody solution (S830, 1:2000; EM48, 1:100, Calbiochem; anti-HRP, 1:1000, MP Biochemicals) for 24 h at 4 °C. Skins were washed 4 times in 0.1% tPBS, re-incubated in secondary antibody (1:10,000) for 24 h at 4 °C, washed for 4 × 10 min in 0.1% tPBS and 5 min in PBS, mounted on glass slides in Vectashield fluorescence mount (Vector Laboratories, CA, US), and analysed at ×63 on a Zeiss Axioplan2 Epifluorescence or Confocal Microscope. Accumulate sizes and peripheral nerve diameters were calculated in Metamorph software (Molecular Devices, CA, USA). The term "aggregate" is used to describe S830 or EM48 immuno-positive structures detectable by light microscopy and encompasses what has been described by others as micro or macro aggregates and/or inclusion bodies. Aggregates were further defined by the following criteria: The diameter of circular and non-circular htt immunoreactive aggregates was measured as the largest cross sectional area. Across our analysis, aggregates fell into two groups. Small aggregates (SAg) measured from 0.7 µm to 1.3 µm in diameter, whereas large aggregates (LAg) were equal to or exceeded 1.3 µm in diameter. For Hoechst chromatin staining, skins were incubated in 1 µg/µl Hoechst in tPBS for 20 min prior to the final PBS wash.

RNA extraction and RT-PCR

For each experiment, 15 HttEx1Q93 larvae, driven with D42-GAL4, were homogenised with Trizol reagent (Invitrogen) to isolate total RNA. RNA was reverse transcribed with iScript cDNA synthesis kit (Biorad). PCR was carried out with HotStar Taq hot start DNA polymerase (Qiagen). HttEx1 – specific primers were P1 (5'-TGGCCG-ACCCTGAAAAGCTG-3') and P2 (5'-TGAGGCAGCAGCGCTGTGC-3'), annealing at 68 °C. RP49 was used as an RNA loading control, as described previously (Tsichritzis et al., 2007). For densitometry analysis, product bands from each of 3 different HttEx1 PCR cycle numbers were expressed as a ratio of RP49 expression, and the average of these ratios used for comparison between 23 °C and 29 °C HttEx1 expression levels.

In vivo axonal transport analysis

Axonal transport analysis was conducted as previously described (Mudher et al., 2004). *Drosophila* L3 larvae were anaesthetised in diethylether vapour for 10 min, immobilised in 1% agarose ventral face up on glass slides, and mounted under coverslips at pressure for analysis. For total accumulate area acquisition, peripheral nerves were analysed between the 2nd and 4th denticular bands. vGFP accumulates were imaged at ×63 on a Axioplan2 Epifluorescence Microscope (Zeiss), and thresholded in Metamorph software (Molecular Devices, CA, USA). Movies of vesicular movement at separate regions of peripheral nerve were captured at ×100 magnification and vesicular movement tracked in Metamorph as previously described (Mudher et al., 2004).

Developmental-, larval locomotion- and statistical analysis

For developmental analysis, single transgenic crosses were established simultaneously with age-matched virgin females. Parents were removed 7d after cross initiation and eclosing adults scored and removed from test vials daily. Line-crossing and contraction tests were conducted as previously described (Mudher et al., 2004). Tests were conducted on a 1 mm bed of 1% agarose in standard *Drosophila* saline. For both tests, larvae were allowed to acclimatise to the testing area for 2 min prior to testing. In the line-crossing assay, the number of lines crossed on a 20 × 20 square grid (10 cm × 10 cm), with the larva starting at the grid's middle point, was counted over 30 s. In the contractions assay, full peristaltic body wall contractions were quantified over 30 s on 1% agarose. For heat shock prior to locomotion tests, larvae were housed individually in plastic Eppendorf vials and incubated at 39 °C for 5 min, before transfer to 1% agarose plates at room temperature for a 1 min cooling period (3 min total) and testing for locomotion ability as described above. For statistical analyses, the unpaired Student's *t*-test was used in Microsoft Excel.

Author's contributions

AM and AW are corresponding authors and contributed equally to this study; CS performed all of the experiments including data analysis and writing the first draft of the paper. TB and DS initiated the development of the HD fly model. LT and LM provided the HttEx1 *Drosophila* lines and supported this study with valuable advice.

Acknowledgments

We would like to thank Gil Bates for providing the htt exon 1 antibody (S830). Thanks go to Vincent O' Connor, Sarah Hands, and Torsten Bossing for discussions and suggestions. This work was funded by the BBSRC (AM, AW, CS) and the MRC (AW).

Appendix A. Supplementary data

Supplementary data associated with this article can be found, in the online version, at doi:10.1016/j.nbd.2009.02.012.

References

- Albin, R.L., Reiner, A., Anderson, K.D., Dure, L.S., Handelin, B., Balfour, R., Whetsell Jr., W.O., Penney, J.B., Young, A.B., 1992. Preferential loss of striato-external pallidal projection neurons in presymptomatic Huntington's disease. *Ann. Neurol.* 31, 425–430.
- Brand, A.H., Perrimon, N., 1993. Targeted gene expression as a means of altering cell fates and generating dominant phenotypes. *Development* 118, 401–415.
- Brown, A., 2003. Axonal transport of membranous and nonmembranous cargoes: a unified perspective. *J. Cell Biol.* 160, 817–821.
- D'Hooge, R., De Deyn, P.P., Verzwijvelen, A., De, B.J., De Potter, W.P., 1990. Storage and fast transport of noradrenaline, dopamine beta-hydroxylase and neuropeptide Y in dog sciatic nerve axons. *Life Sci.* 47, 1851–1859.

- DiFiglia, M., Sapp, E., Chase, K.O., Davies, S.W., Bates, G.P., Vonsattel, J.P., Aronin, N., 1997. Aggregation of huntingtin in neuronal intranuclear inclusions and dystrophic neurites in brain. *Science* 277, 1990–1993.
- Gidalevitz, T., Ben-Zvi, A., Ho, K.H., Brignull, H.R., Morimoto, R.I., 2006. Progressive disruption of cellular protein folding in models of polyglutamine diseases. *Science* 311, 1471–1474.
- Gunawardena, S., Goldstein, L.S., 2005. Polyglutamine diseases and transport problems: deadly traffic jams on neuronal highways. *Arch. Neurol.* 62, 46–51.
- Gunawardena, S., Her, L.S., Brusch, R.G., Laymon, R.A., Niesman, I.R., Gordesky-Gold, B., Sintasath, L., Bonini, N.M., Goldstein, L.S., 2003. Disruption of axonal transport by loss of huntingtin or expression of pathogenic polyQ proteins in *Drosophila*. *Neuron* 40, 25–40.
- Hurd, D.D., Saxton, W.M., 1996. Kinesin mutations cause motor neuron disease phenotypes by disrupting fast axonal transport in *Drosophila*. *Genetics* 144, 1075–1085.
- Katsuno, M., Adachi, H., Minamiyama, M., Waza, M., Tokui, K., Banno, H., Suzuki, K., Onoda, Y., Tanaka, F., Doyu, M., Sobue, G., 2006. Reversible disruption of dynactin 1-mediated retrograde axonal transport in polyglutamine-induced motor neuron degeneration. *J. Neurosci.* 26, 12106–12117.
- Lee, W.C., Yoshihara, M., Littleton, J.T., 2004. Cytoplasmic aggregates trap polyglutamine-containing proteins and block axonal transport in a *Drosophila* model of Huntington's disease. *Proc. Natl. Acad. Sci. U. S. A.* 101, 3224–3229.
- Li, H., Li, S.H., Cheng, A.L., Mangiarini, L., Bates, G.P., Li, X.J., 1999. Ultrastructural localization and progressive formation of neuropil aggregates in Huntington's disease transgenic mice. *Hum. Mol. Genet.* 8, 1227–1236.
- Li, H., Li, S.H., Yu, Z.X., Shelbourne, P., Li, X.J., 2001. Huntingtin aggregate-associated axonal degeneration is an early pathological event in Huntington's disease mice. *J. Neurosci.* 21, 8473–8481.
- Mangiarini, L., Sathasivam, K., Seller, M., Cozens, B., Harper, A., Hetherington, C., Lawton, M., Trotter, Y., Leach, H., Davies, S.W., Bates, G.P., 1996. Exon 1 of the HD gene with an expanded CAG repeat is sufficient to cause a progressive neurological phenotype in transgenic mice. *Cell* 87, 493–506.
- Morfino, G., Pigino, G., Szebenyi, G., You, Y., Pollema, S., Brady, S.T., 2006. JNK mediates pathogenic effects of polyglutamine-expanded androgen receptor on fast axonal transport. *Nat. Neurosci.* 9, 907–916.
- Mudher, A., Shepherd, D., Newman, T.A., Mildren, P., Jukes, J.P., Squire, A., Mears, A., Drummond, J.A., Berg, S., MacKay, D., et al., 2004. GSK-3 β inhibition reverses axonal transport defects and behavioural phenotypes in *Drosophila*. *Mol. Psychiatry* 9, 522–530.
- Orr, A.L., Li, S., Wang, C.E., Li, H., Wang, J., Rong, J., Xu, X., Mastroberardino, P.G., Greenamyre, J.T., Li, X.J., 2008. N-terminal mutant huntingtin associates with mitochondria and impairs mitochondrial trafficking. *J. Neurosci.* 28, 2783–2792.
- Phelps, C.B., Brand, A.H., 1998. Ectopic gene expression in *Drosophila* using GAL4 system. *Methods* 14, 367–379.
- Reiner, A., Albin, R.L., Anderson, K.D., D'Amato, C.J., Penney, J.B., Young, A.B., 1988. Differential loss of striatal projection neurons in Huntington disease. *Proc. Natl. Acad. Sci. U. S. A.* 85, 5733–5737.
- Romero, E., Cha, G.H., Verstreken, P., Ly, C.V., Hughes, R.E., Bellen, H.J., Botas, J., 2008. Suppression of neurodegeneration and increased neurotransmission caused by expanded full-length huntingtin accumulating in the cytoplasm. *Neuron* 57, 27–40.
- Sapp, E., Penney, J., Young, A., Aronin, N., Vonsattel, J.P., DiFiglia, M., 1999. Axonal transport of N-terminal huntingtin suggests early pathology of corticostriatal projections in Huntington disease. *J. Neuropathol. Exp. Neurol.* 58, 165–173.
- Sathasivam, K., Woodman, B., Mahal, A., Bertaux, F., Wanker, E.E., Shima, D.T., Bates, G.P., 2001. Centrosome disorganization in fibroblast cultures derived from R6/2 Huntington's disease (HD) transgenic mice and HD patients. *Hum. Mol. Genet.* 10, 2425–2435.
- Steffan, J.S., Bodai, L., Pallos, J., Poelman, M., McCampbell, A., Apostol, B.L., Kazantsev, A., Schmidt, E., Zhu, Y.Z., Greenwald, et al., 2001. Histone deacetylase inhibitors arrest polyglutamine-dependent neurodegeneration in *Drosophila*. *Nature* 413, 739–743.
- Szebenyi, G., Morfino, G.A., Babcock, A., Gould, M., Selkoe, K., Stenoien, D.L., Young, M., Faber, P.W., MacDonald, M.E., McPhaul, M.J., Brady, S.T., 2003. Neuropathogenic forms of huntingtin and androgen receptor inhibit fast axonal transport. *Neuron* 40, 41–52.
- The Huntington's Disease Collaborative Research Group, 1993. A novel gene containing a trinucleotide repeat that is expanded and unstable on Huntington's disease chromosomes. *Cell* 72, 971–983.
- Trushina, E., Dyer, R.B., Badger, J.D., Ure, D., Eide, L., Tran, D.D., Vrieze, B.T., Legendre-Guillemin, V., McPherson, P.S., Mandavilli, et al., 2004. Mutant huntingtin impairs axonal trafficking in mammalian neurons in vivo and in vitro. *Mol. Cell. Biol.* 24, 8195–8209.
- Tsichritzis, T., Gaentzsch, P.C., Kosmidis, S., Brown, A.E., Skoulakis, E.M., Ligoxygakis, P., Mosialos, G., 2007. A *Drosophila* ortholog of the human cylindromatosis tumor suppressor gene regulates triglyceride content and antibacterial defense. *Development* 134, 2605–2614.
- van Dellen, A., Blakemore, C., Deacon, R., York, D., Hannan, A.J., 2000. Delaying the onset of Huntington's in mice. *Nature* 404, 721–722.
- Vonsattel, J.P., Myers, R.H., Stevens, T.J., Ferrante, R.J., Bird, E.D., Richardson Jr., E.P., 1985. Neuropathological classification of Huntington's disease. *J. Neuropathol. Exp. Neurol.* 44, 559–577.
- Wade, A., Jacobs, P., Morton, A.J., 2008. Atrophy and degeneration in sciatic nerve of presymptomatic mice carrying the Huntington's disease mutation. *Brain Res.* 1188, 61–68.
- Wexler, N.S., Lorimer, J., Porter, J., Gomez, F., Moskowitz, C., Shackell, E., Marder, K., Penchaszadeh, G., Roberts, S.A., Gayan, J., et al., 2004. Venezuelan kindreds reveal that genetic and environmental factors modulate Huntington's disease age of onset. *Proc. Natl. Acad. Sci. U. S. A.* 101, 3498–3503.
- Wolfgang, W.J., Miller, T.W., Webster, J.M., Huston, J.S., Thompson, L.M., Marsh, J.L., Messer, A., 2005. Suppression of Huntington's disease pathology in *Drosophila* by human single-chain Fv antibodies. *Proc. Natl. Acad. Sci. U. S. A.* 102, 11563–11568.
- Zhou, H., Cao, F., Wang, Z., Yu, Z.X., Nguyen, H.P., Evans, J., Li, S.H., Li, X.J., 2003. Huntingtin forms toxic NH₂-terminal fragment complexes that are promoted by the age-dependent decrease in proteasome activity. *J. Cell Biol.* 163, 109–118.